

Published in final edited form as:

J Am Chem Soc. 2011 June 8; 133(22): 8525–8527. doi:10.1021/ja202818v.

Chelated Ruthenium Catalysts for Z-Selective Olefin Metathesis

Koji Endo and Robert H. Grubbs*

Arnold and Mabel Beckman Laboratory of Chemical Synthesis, Division of Chemistry and Chemical Engineering, California Institute of Technology, Pasadena, California 91125, United States

Abstract

We report the development of ruthenium-based metathesis catalysts with chelating *N*-heterocyclic carbene (NHC) ligands which catalyze highly *Z*-selective olefin metathesis. A very simple and convenient synthetic procedure of such a catalyst has been developed. An intramolecular C-H bond activation of the NHC ligand, which is promoted by anion ligand substitution, forms the appropriate chelate for stereo- controlled olefin metathesis.

Based on the continued development of well-defined catalysts, olefin metathesis has emerged as a valuable synthetic method for the formation of carbon-carbon double bonds.¹ Among the frontiers of catalyst development has been the quest for *Z*-selective olefin metathesis catalysts which would enable access to complex natural products² and stereo-regular unique polymers.³ Specifically, the use of *Z*-selective catalysts in olefin cross-metathesis (CM) represents a promising and useful methodology in organic chemistry. However, due to the thermodynamic nature of metathesis,⁴ most catalysts give a higher proportion of the thermodynamically favored *E* olefin isomer. This fundamental aspect of olefin metathesis has limited its applications in some areas of chemistry.

Recently, some ruthenium-based catalysts which showed enhanced *Z*-selectivity have been reported, however, their selectivity is still not satisfactory for precisely stereo-controlled syntheses.⁵ On the other hand, recently developed molybdenum- and tungsten- based catalysts have shown outstanding *Z*-selectivity in CM² and metathesis homocoupling⁶ of terminal olefins. In particular, a bulky aryloxy substituted molybdenum catalyst afforded the cross-coupled product of enol ether and allylbenzene with 98% of the *Z* isomer. As has been demonstrated in the past, the ruthenium- and molybdenum-based systems show significant differences in selectivities and utility.⁷

For general use, metathesis catalysts should be not only tolerant towards various functional groups and impurities in reaction media, but also readily synthesized from common reagents by simple reaction steps. Here, we report chelated ruthenium catalysts, which catalyze highly *Z*-selective olefin metathesis, and their facile synthetic preparation.

We chose [H₂IMes₂]RuCl₂[=CH-*o*-(*O*^{*i*}Pr)C₆H₄] (**1a**, H₂I = imidazolidinylidene, Mes = mesityl) and the bulkier [H₂IMesAdm]-RuCl₂[=CH-*o*-(*O*^{*i*}Pr)C₆H₄] (**1b**, Adm = 1-adamantyl) as precursors. **1b** was readily synthesized from commercially available **2** in excellent yield (Scheme 1).⁸

rhg@caltech.edu.

Supporting Information Available: Experimental procedures and X-ray data. This material is available free of charge via the Internet at <http://pubs.acs.org>.

Reaction of **1a** with excess silver pivalate resulted in the formation of **3a**, which was only observed at early reaction times.⁹ Subsequent intramolecular C-H bond activation at the methyl position of the mesityl group resulted in the formation of **4a** with concomitant release of pivalic acid (Scheme 2). Such intramolecular C-H bond activations assisted by carboxylate ligands have been reported in other organometallic complexes.¹⁰ Based on these previous reports, a plausible mechanism for the C-H bond activation in **3a** contains 6-membered (**A**) or 4-membered (**B**) transition state shown in Figure 1. It should be noted that no other anionic ligands including sulfonate,^{5b} phosphonate,^{5b} and trifluoroacetate¹¹ promote such intramolecular C-H bond activation in **1a**. An X-ray crystal structure of **4a** clearly indicates the C-H bond activation at the NHC ligand and subsequent formation of the 6-membered chelated complex (Figure 2).

When **1b** was reacted with excess silver pivalate, C-H bond activation occurred at the adamantyl group, which resulted in the formation of the 5-membered chelate complex [(C₁₀H₁₄)H₂[Mes]-RuCl₂[=CH-*o*-(O^{*i*}Pr)C₆H₄] (**4b**) (Scheme 3). A dicarboxylate complex was not detected as the C-H bond activation reaction of **1b** was too fast, but observation of pivalic acid suggests the same reaction mechanism of intramolecular C-H bond activation. The C-H bond activation at the adamantyl group and the fast reaction may be attributed to the ligand geometry in **1b**. An X-ray crystal structure of **1b** showed that the adamantyl group is proximal to a vacant coordination site where the C-H bond activation is supposed to occur and the distance between ruthenium and C12, where a new bond forms after C-H bond activation, is relatively short (2.80 Å).¹² The molecular structure of **4b** determined by X-ray crystallography revealed an adamantyl contained chelate which confirmed the intramolecular C-H bond activation at the adamantyl group (Figure 3).

Complexes having chelating NHC ligand derived from intramolecular C-H bond activation have been reported.¹³ Most of them were formed during catalyst decomposition pathway and none have been reported to have catalytic activity. We investigated at first whether **4a** and **4b** were still 'active' as olefin meta thesis catalysts, testing them in standard ring closing metathesis (RCM) of diethyldiallyl malonate (**5**)¹⁴ and ring opening metathesis polymerization (ROMP) of norbornene (**7**). As shown in Figure 4, both **4a** and **4b** were metathesis active in the RCM reaction although activities were lower than **1a**. Because of catalyst decomposition, the conversion by **4a** was limited to ca. 14%. On the other hand, **4b** was able to achieve almost full conversion at higher temperature (70 °C). In the ROMP of **7** affording polynorbornene (**8**), both **4a** and **4b** also showed high activities at the presented conditions.¹⁶

Encouraged by the results of the standard metathesis assays, we then tested the CM of allylbenzene (**9**) and *cis*-1,4-diacetoxy-2-butene (**10**).¹⁴ Selected data of the CM are summarized in Table 1. Surprisingly, **4a** and **4b** gave a much lower *E/Z* ratio of the cross-coupled product (**11**) (entry 1 and 2) compared to their parent non-chelate catalysts (entry 6 and 7). The *E/Z* ratio of 0.12 (90% *Z* isomer) achieved by **4b** is among the lowest reported for ruthenium- based olefin metathesis catalysts. In addition to this, the homocoupled product (**12**) afforded by **4b** also showed significantly low *E/Z* ratio (*E/Z* = 0.06, 95% *Z* isomer). The conversion to **11** was improved under THF reflux condition maintaining excellent *Z*-selectivity (entry 3). This was probably a result of more efficient removal of ethylene which was generated during the course of reaction. Unexpectedly, addition of water led to higher conversions and selectivity for the *Z* olefin products (entry 4). This result implies not only that water can be used to optimize reaction conditions but also that **4b** is tolerant towards water in organic solvent. Thus, dry solvent is not necessary for **4b** in olefin metathesis reactions. This feature enables easy use of the catalyst in common organic syntheses and polymer syntheses without strict reaction conditions. However, **4b** decomposed immediately when exposed to oxygen in solution, meaning that degassing of

solvent is required to achieve high conversion. Notably, the reaction was reproducible on a synthetic scale (mmol scale, entry 5).

In summary, we have demonstrated the utility of chelated ruthenium catalyst for *Z*-selective olefin cross-metathesis reactions. The *Z*-selectivity achieved by **4b** is the best among reported ruthenium- based catalysts and comparable to the molybdenum- and tungsten-based catalysts. Notably, this is the first time that *Z*-selectivity in the cross-metathesis of two different olefins has been demonstrated using a ruthenium-based catalyst. The ruthenium catalyst is readily synthesized from common reagents via simple reaction steps and is stable in the presence of water which should promote its application in precisely stereo-controlled organic and polymer syntheses.

Supplementary Material

Refer to Web version on PubMed Central for supplementary material.

Acknowledgments

We thank Mr. B. K. Keitz, Mr. M. B. Herbert and Dr. P. Teo for helpful discussions and suggestions for this work, Materia, Inc. for the generous donation of catalysts and Dr. M. W. Day and Mr. L. M. Henling for X-ray crystallography. The Bruker KAPPA APEXII X-ray diffractometer was purchased via an NSF CRIF:MU award to the California Institute of Technology, CHE-0639094. This work was financially supported by National Institutes of Health (NIH 5R01GM031332-27) and Mitsui Chemicals, Inc.

References

1. (a) Fürstner A. *Angew Chem Int Ed.* 2000; 39:3012–3043. (b) Trnka TM, Grubbs RH. *Acc Chem Res.* 2001; 34:18–29. [PubMed: 11170353] (c) Schrock RR. *Chem Rev.* 2002; 102:145–179. [PubMed: 11782131] (d) Schrock RR, Hoveyda AH. *Angew Chem Int Ed.* 2003; 42:4592–4633. (e) Samojłowicz C, Bieniek M, Grela K. *Chem Rev.* 2009; 109:3708–3742. [PubMed: 19534492] (f) Vougioukalakis G, Grubbs RH. *Chem Rev.* 2010; 110:1746–1787. [PubMed: 20000700]
2. Meek SJ, O'Brien RV, Llaveria J, Schrock RR, Hoveyda AH. *Nature.* 2011; 471:461–466. [PubMed: 21430774]
3. (a) Flook MM, Jiang AJ, Schrock RR, Muller P, Hoveyda AH. *J Am Chem Soc.* 2009; 131:7962–7963. [PubMed: 19462947] (b) Flook MM, Gerber LCH, Debelouchina GT, Schrock RR. *Macromolecules.* 2010; 43:7515–7522. [PubMed: 21499508] (c) Torker S, Müller A, Chen P. *Angew Chem Int Ed.* 2010; 49:3762–3766. (d) Flook MM, Ng VWL, Schrock RR. *J Am Chem Soc.* 2011; 132:1784–1786.
4. Grubbs, RH., editor. *Handbook of Metathesis.* Wiley-VCH; Weinheim: 2003. p. s1-3.
5. (a) Rosen EL, Sung DH, Chen Z, Lynch VM, Bielawski CW. *Organometallics.* 2010; 29:250–256. (b) Teo P, Grubbs RH. *Organometallics.* 2010; 29:6045–6050.
6. (a) Jiang AJ, Zhao Y, Schrock RR, Hoveyda AH. *J Am Chem Soc.* 2009; 131:16630–16631. [PubMed: 19919135] (b) Marinescu SC, Schrock RR, Müller P, Takase MK, Hoveyda AH. *Organometallics.* 2011; 30:1780–1782. [PubMed: 21686089]
7. Cortez GA, Baxter CA, Schrock RR, Hoveyda AH. *Org Lett.* 2007; 9:2871–2874. [PubMed: 17585770]
8. Jafarpour L, Hillier AC, Nolan SP. *Organometallics.* 2002; 21:442–444.
9. **3a** was detected by ¹H NMR and FD-MS. See details in the Supporting Information.
10. (a) Davies DL, Donald SMA, Al-Duaij O, Macgregor SA, Pölleth M. *J Am Chem Soc.* 2006; 128:4210–4211. [PubMed: 16568979] (b) Li L, Brennessel WW, Jones WD. *J Am Chem Soc.* 2008; 130:12414–12419. [PubMed: 18714995] (c) Li L, Brennessel WW, Jones WD. *Organometallics.* 2009; 28:3492–3500. (d) Tsurugi H, Fujita S, Choi G, Yamagata T, Ito S, Miyasaka H, Mashima K. *Organometallics.* 2010; 29:4120–4129.
11. Krause JO, Nuyken O, Wurst K, Buchmeiser MR. *Chem Eur J.* 2004; 10:777–784.
12. For X-ray crystal structure and selected bond length of **1b**, see the Supporting Information.

13. (a) Trnka TM, Morgan JP, Sanford MS, Wilhelm TE, Scholl M, Choi TL, Ding S, Day MW, Grubbs RH. *J Am Chem Soc.* 2003; 125:2546–2558. [PubMed: 12603143] (b) Leitao EM, Dubberley SR, Piers WE, Wu Q, McDonald R. *Chem Eur J.* 2008; 14:11565–11572.
14. Ritter T, Hejl A, Wenzel AG, Funk TW, Grubbs RH. *Organometallics.* 2006; 25:5740–5745.
15. The RCM data was referred to ref. 14.
16. For the reaction conditions and results, see the Supporting Information.

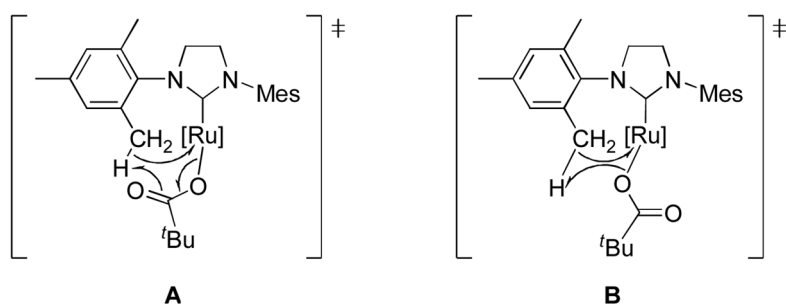


Figure 1.
Plausible transition states of the intramolecular C-H bond activation in **3a**.

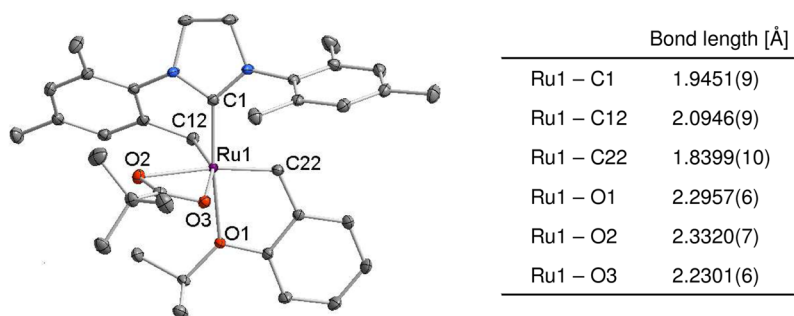


Figure 2. X-ray crystal structure and selected bond length of **4a** are shown. Displacement ellipsoids are drawn at 50% probability. For clarity, hydrogen atoms have been omitted.

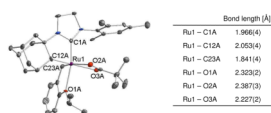


Figure 3. X-ray crystal structure and selected bond length of **4b** are shown. Displacement ellipsoids are drawn at 50% probability. For clarity, hydrogen atoms have been omitted.

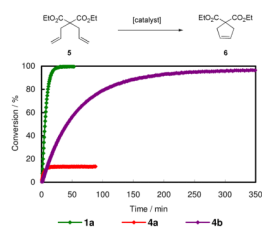
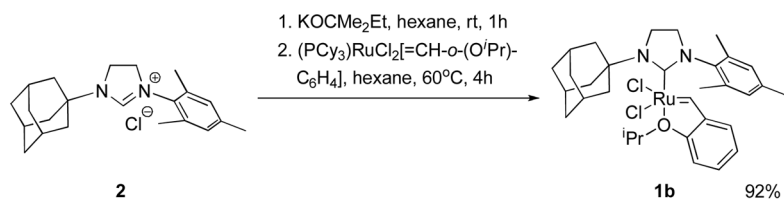
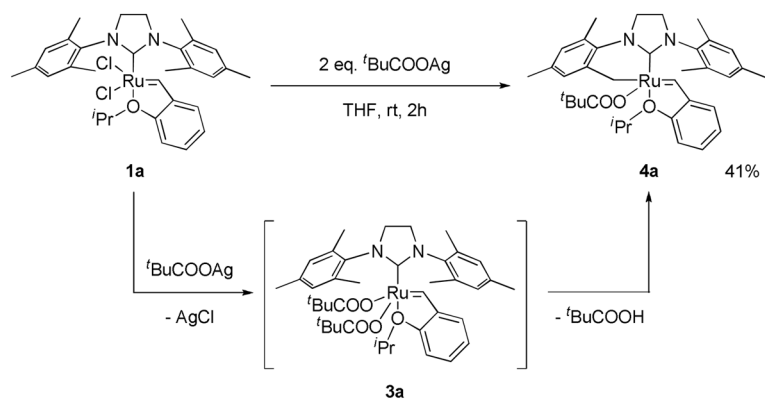


Figure 4.

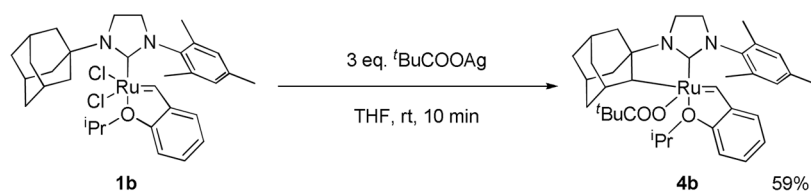
Plot of conversion versus time for the RCM of **5**. Reaction conditions were as follows; **1a**¹⁵: 1.0 mol % catalyst, 0.1 M substrate, 30 °C, CD₂Cl₂; **4a**: 1.0 mol % catalyst, 0.1 M substrate, 30 °C, C₆D₆; **4b**: 5.0 mol % catalyst, 0.1 M substrate, 70 °C, C₆D₆.



Scheme 1.
Synthesis of **1b**

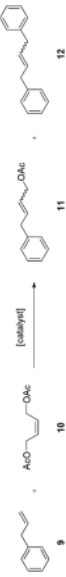


Scheme 2.
Synthesis of 4a



Scheme 3.
Synthesis of 4b

Table 1

CM of **9** and **10**^a


entry	catalyst	catalyst loading mol % ^b	solvent	temp °C	time min	conversion ^c %	<i>E/Z</i> ^d	conversion ^e %	<i>E/Z</i> ^d
1	4a	2.5	C ₆ H ₆	23	10	57.5	1.44	3.3	1.21
2	4b	5.0	C ₆ H ₆	70	60	57.4	1.44	3.0	0.69
3	4b	5.0	THF	(reflux)	240	32.5	0.13	24.8	0.07
4	4b	5.0	THF/H ₂ O ^e	(reflux)	240	36.4	0.12	26.0	0.06
5 ^f	4b	5.0	THF/H ₂ O ^e	(reflux)	240	59.5	0.19	31.6	0.04
6	1a	2.5	C ₆ H ₆	23	1	64.4	0.14	28.6	0.03
7	1b	2.5	C ₆ H ₆	23	30	61.6 ^g	0.14	NA ^h	0.03
					1	69.7	10.5	5.9	5.22
					30	66.3	10.7	10.2	6.86
					1	0.15	3.10	NA ⁱ	NA ⁱ
					30	0.23	2.90	NA ⁱ	NA ⁱ

^a All reactions unless otherwise stated were carried out using 0.20 mmol of **9**, 0.40 mmol of **10** and 0.10 mmol of tridecane (internal standard for GC analysis) in 1.0 ml of solvent.^b Based on **9**.^c Conversion of **9** to the product determined by GC analysis.^d Molar ratio of *E* isomer and *Z* isomer of the product determined by GC analysis.^e THF : H₂O = 1 : 1 (by volume).^f The reaction was carried out using 1.0 mmol of **9**, 2.0 mmol of **10** and 0.050 mmol of catalyst in 5.0 ml of solvent.^g Isolated yield.^h **12** was obtained with impurities.ⁱ GC signal of **12** was too small to quantify.